NATURAL RESOURCE MODELING
Volume 24, Number 1, February 2011

DERIVATION OF TWO WELL-BEHAVED THEORETICAL CONTAGION INDICES AND THEIR SAMPLING PROPERTIES AND APPLICATION FOR ASSESSING FOREST LANDSCAPE DIVERSITY

BERNARD R. PARRESOL*
USDA Forest Service, Southern Research Station, 200 WT Weaver Blvd., Asheville, NC 28804-3454
E-mail: bparresol@fs.fed.us

ABSTRACT. Studies of spatial patterns of landscapes are useful to quantify human impact, predict wildlife effects, or describe variability of landscape features. A common approach to identify and quantify landscape structure is with a landscape scale model known as a contagion index. A contagion index quantifies two distinct components of landscape diversity: composition and configuration. Some landscape ecologists promote the use of relative contagion indices. It is demonstrated that relativized contagion indices are mathematically untenable. Two new theoretical contagion indices, Γ_1 and Γ_2, are derived using a mean value approach (i.e., statistical expected value) instead of entropy. Behavior of Γ_1 and Γ_2 was investigated with simulated random, uniform, and aggregated landscapes. They are shown to be well-behaved and sensitive to composition and configuration. Distributional properties of $\hat{\Gamma}_1$ and $\hat{\Gamma}_2$ are derived. They are shown to be asymptotically unbiased, consistent, and asymptotically normally distributed. Variance formulas for $\hat{\Gamma}_1$ and $\hat{\Gamma}_2$ are developed using the delta method. The new index models are used to examine landscape diversity on three physiographic provinces in Alabama by analyzing the pattern and changes in forest cover types over the recent past. In comparing $\hat{\Gamma}_1$ and $\hat{\Gamma}_2$, use of $\hat{\Gamma}_1$ in analysis of variance gave a more conservative test of contagion.

KEY WORDS: Concentration, delta method, entropy, expected value, forest cover types, geometric distribution, physiographic provinces, simulated landscapes.

*Corresponding author. Bernard R. Parresol, USDA Forest Service, Southern Research Station, 200 WT Weaver Blvd., Asheville, NC 28804-3454, e-mail: bparresol@fs.fed.us.

Received by the editors on 26th January, 2010. Accepted 9th September, 2010.

1. Introduction

1.1. Landscapes and contagion. Landscape diversity refers to the various ecosystems (including human, e.g., cities, farm country, etc.) within a large area. The structure observed in landscapes result from complex interactions among physical, biological, and social forces. Most landscapes have been altered by human land use, and the resulting landscape mosaic is a mixture of natural and human-managed patches that vary in size, shape, and arrangement (Burgess and Sharpe [1981]). A commonly used tool for measuring spatial structure on landscapes is the contagion index.

A landscape contagion index is a quantitative metric, a single statistic applied on a broad spatial scale in which two distinct components are confounded: composition and configuration. Composition refers to both the total number of land-cover categories or "patch" types and their relative proportions in the landscape, whereas configuration refers to the spatial pattern of patches in the landscape (Li and Reynolds [1993]). Contagion, as defined by O'Neill et al. [1988], measures the extent to which landscape elements are aggregated or clumped. Higher values of contagion generally result from landscapes with a few large, contiguous patches, whereas lower values usually characterize landscapes with many small patches. Also, holding the number of categories more or less constant, contagion values, in general, should decrease as category proportions become more even.

From the above definitions, it is obvious that landscape contagion, as a property, has a reverse scale from that of species diversity. A single-species community has no diversity while an infinite-species community has maximum diversity. The exact opposite is true from a contagion viewpoint. That is, a single-category landscape has maximum contagion whereas an infinite-category landscape has no contagion. In this regard, contagion equates to spatial autocorrelation. If categories are not correlated in space (i.e., autocorrelation ≈ 0), then there is greater uncertainty at any point on the identity of surrounding neighbors.

Since its introduction over two decades ago, the contagion index has been used extensively in the analysis and modeling of landscapes and ecosystems. It has been used to detect changes in spatial patterns and

structure across a variety of landscapes around the globe (e.g., Turner and Ruscher [1988], Dale et al. [1993, 1994], Sachs et al. [1998], Shi et al. [2008]). Contagion has been used in ecological risk assessment (Graham et al. [1991]). Gustafson and Parker [1992] used contagion to analyze the relationship between land-cover proportions and spatial pattern. Contagion is currently being used to study and model land-use dynamics in urban areas (see, e.g., Dietzel et al. [2005], Haack and Rafter [2006], Yu and Ng [2006], Thapa and Murayama [2008]). According to Alberti [2009, p. 116], dispersion of urban areas can be effectively measured using contagion and aggregation indices.

To date, only a handful of (relativized) contagion indices have been proposed (O'Neill et al. [1988], Li and Reynolds [1993], Riitters et al. [1996]). Researchers such as Frohn [1998, p. 14] and Ricotta et al. [2003] have raised concern over the effects of varying composition on these contagion indices. In no cases have distributional properties been examined. As a statistic, a contagion index is limited if it cannot be used in making comparisons of diversities among different landscapes or the same landscape through time based on sample data. The sampling properties of a landscape index must be known before one can construct an appropriate test. Is the index unbiased? Consistent? Can the variance be computed or approximated? Is the sample distribution normal? A formal investigation needs to be done to answer these questions.

1.2. Forested landscapes. Forest landscape management is based on the premise that resource flows as well as biodiversity levels and ecosystem processes are determined by the array and spatial arrangement of forest conditions, i.e., spatial structure, and its change over time (Waring and Running [1998]). Forested landscapes are normally categorized into forest cover types (Fralish and Franklin [2002]). Several forest cover type classifications are currently used within the forestry profession, the two most commonly used in the United States are the Society of American Foresters system (Eyre [1980]) and the USDA Forest Service-Forest Inventory and Analysis (FIA) system (Miles et al. [2001]). Progress has been made at the regional scale to map general forest cover types from remotely sensed data (e.g., Zhu and Evans [1994], Sasaki et al. [2001], Kachmar et al. [2005]). However, in the United States, FIA sample-based forest survey data are widely

available for specific forest cover type mapping going back to the 1930s, giving us the ability to look back historically at landscape diversity.

Geologic landforms have been mapped and classified into physiographic provinces and are readily available for input into a geographic information system (GIS). With the digitized maps and the FIA data, a unique opportunity exists to apply a contagion index and distribution theory to characterize and compare forest cover type diversity on landscape scale physiographic provinces.

1.3. Objectives. This paper develops new contagion indices and provides a statistical basis for their use in hypothesis testing. They are applied to a particular forest region of interest. There were a number of specific objectives of this research. First, to demonstrate, using simulated landscapes under three scenarios that relativized contagion indices possess mathematically undesirable qualities. This conveys the need for new indices that overcome the illogical behavior inherent in relativized indices. Second, using statistical expected values as an alternative to the principle of entropy,[1] two indices are derived that exhibit desirable mathematical behavior under the same scenarios where relativized contagion failed. Third, to study the sampling properties of the new contagion indices Γ_1 and Γ_2. And fourth, apply the new indices, using FIA data on forest cover types, for comparing three landscape-level physiographic provinces of Alabama: (i) Great Appalachian Valley Province, (ii) Blue Ridge-Talladega Mountain Province, and (iii) Piedmont Province.

2. Previous contagion indices. O'Neill et al. [1988] developed two landscape scale measures based on information theory. Their first index (D_1) is a measure of dominance. Their second index quantifies the extent to which different types are intermingled. It is given by

$$D_2 = 2n\ln(n) + \sum_{i=1}^{n}\sum_{j=1}^{n} p_{ij}\ln(p_{ij}), \tag{1}$$

where p_{ij} is the probability that a grid cell of land cover i is found adjacent[2] (rook's rule) to a grid cell of land cover j, and n is the total number of land-cover categories (patch types) in a particular landscape.

Li and Reynolds [1993] showed that D_2 is insensitive to changes in spatial pattern. This is because of an error, which they identified, in the formulation of the index. Li and Reynolds defined relative contagion (RC) as

$$RC = 1 - EE/EE_{\max}, \tag{2}$$

where EE denotes the entropy value. The well-known measure of entropy for categorical data, derived by Shannon (Shannon and Weaver [1949]), is $-\sum p_i \ln(p_i)$. Based on equation (2), Li and Reynolds gave two new indices. The first is

$$RC_1 = 1 + \frac{\sum_{i=1}^{n}\sum_{j=1}^{n} \tilde{p}_{ij} \ln(\tilde{p}_{ij})}{n \ln(n)}, \tag{3}$$

where $\tilde{p}_{ij} = p_{j/i} = N_{ij}/N_i$, $p_{j/i}$ is the conditional probability, N_{ij} is the number of joins between pixels of patch types i and j (rook's rule), and N_i is the total number of joins between pixels of patch type i and all patch types (including patch i itself). With this definition of $\tilde{p}_{ij}$ they proved $EE_{\max} = n \ln(n)$. Their second index is

$$RC_2 = 1 + \frac{\sum_{i=1}^{n}\sum_{j=1}^{n} p_{ij} \ln(p_{ij})}{2 \ln(n)}, \tag{4}$$

where $p_{ij} = p_i \cdot p_{j/i}$ and p_i is the probability that a randomly chosen pixel belongs to patch type i (estimated by the proportion of patch type i). With this definition of p_{ij}, Li and Reynolds proved $EE_{\max} = 2 \ln(n)$. The error in D_2 was the use of $2n \ln(n)$ instead of the correct $EE_{\max}$ of $2 \ln(n)$. Thus D_2 has a lower limit of 0 and no upper limit, but RC_1 and RC_2 range from 0 to 1.

Riitters et al. [1996] examined what happens to the maximum possible entropy value for different ways of tabulating attribute (patch type) adjacencies—with and without preserving the order of pixels in pairs. They showed when pixel order is preserved, the maximum entropy value is $2 \ln(n)$ and the index RC_2 is obtained. When pixel order

is not preserved, $EE_{\max} = \ln(n^2 + n) - \ln(2)$ and a new index results:

$$RC_{\text{unordered}} = 1 + \frac{\sum_{q=1}^{n_a} p_q \ln(p_q)}{\ln(n^2 + n) - \ln(2)}, \tag{5}$$

where $p_q = f_q/n_p$, f_q is the frequency of pixel pairs that are of attribute adjacency type q, and n_p is the total number of pixel pairs in the map.

3. The problem with relative indices of contagion. For an index to be appropriate, its behavior must follow the precepts of its definition. In the case of relativized contagion, it is easy to demonstrate illogical behavior. Simulated landscapes can be used to formally investigate the behavior of the indices reviewed in Section 2.

3.1. Simulated landscapes

3.1.1. *Increasing gradient of evenness.* A series of simulated landscapes, similar to that used by Li and Reynolds [1993], was generated with different spatial configurations (random, uniform, and clustered) and numbers of patch types (from 2 to 10), with an increasing gradient of evenness of the proportions of patch types. A simple 0 to 1 scaled measure of evenness is given by (Turner [1989])

$$RE = \frac{-\ln\left(\sum_{i=1}^{n} p_i^2\right)}{\ln(n)}, \tag{6}$$

where p_i is the proportion of the landscape in patch type i and RE (relative evenness) approaching 0 means increasing unevenness of the n categories and $RE = 1$ means all categories occur in equal proportion.

For each of the three configurations, nine maps were generated. The first map had two patch types covering 90% and 10%, respectively. The second map had three patch types covering 80%, 10%, and 10%, respectively. The third map had patch type 1 covering 70% and the remaining three types covering 10% each, and so on. The ninth map contained 10 patch types each covering 10% of the surface area. The

rationale behind this scheme is to have a coverage of points between the extremes of high contagion to low contagion.

The outlined scheme resulted in 27 simulated landscapes, nine for each spatial configuration. For each index, the computed values were plotted over number of patch types by spatial configuration, which gives a graph showing three lines, each determined by nine points. The plots show the sensitivity of the indices to changing numbers of categories/evenness (i.e., composition) and spatial configurations.

3.1.2. *Same degree of evenness.* As a second approach to looking at the behavior of the indices, another series of simulated landscapes was constructed for random, uniform, and clustered spatial configurations and numbers of patch types (from 2 to 10) but with completely even proportions of patch types. That is, for two patch types each type occupied half of the area, for three patch types each type occupied one-third of the area, and so on ($RE \approx 1$ for each map). Again, this resulted in 27 simulated landscapes, nine for each spatial configuration. A plot of the index values computed on these maps show if the indices, proportions being equal, are sensitive to increasing number of categories under different spatial configurations.

3.2. The case against relative contagion

3.2.1. *Same degree of evenness.* Consider the graph of RC_2 values (Figure 1) from the 27 landscapes with $RE \approx 1$ (i.e., same degree of evenness). The three spatial configurations separate out very distinctly, but the three lines are essentially flat, showing that RC_2 is completely insensitive to changes in number of patch types on the landscape when category proportions are equal. The other relative contagion indices behaved similarly. What does this mean?

Figure 1 reveals that RC_2 is measuring something other than contagion. For each value along the x-axis, RE is constant at its maximum value of 1. There is a direct parallel between the constancy of RE and the constancy of RC_2 for each spatial configuration. It appears RC_2 is measuring evenness.

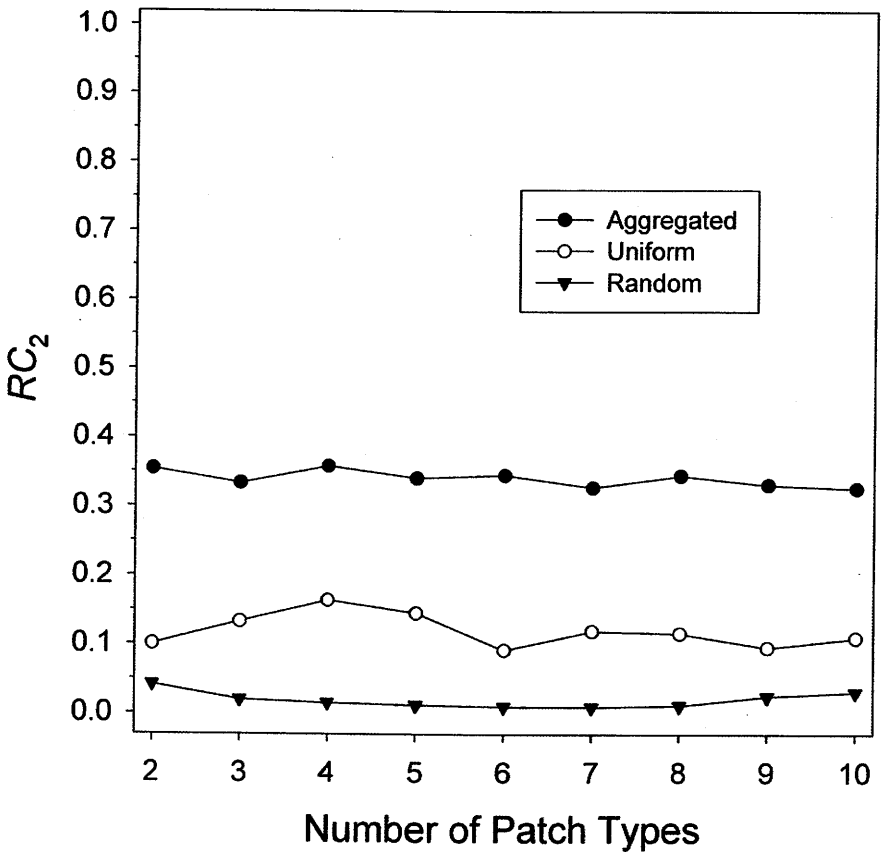

FIGURE 1. Trend lines showing the relationship between RC_2 and the two controlled variables: spatial pattern and number of patch types. Relative evenness ≈ 1 at each point along the x-axis.

3.2.2. *Uniform landscapes—disparate evenness.* To illustrate this point further, consider the three uniform landscapes in Figure 2. Conceptually, as more patch types are included on a landscape, contagion should decrease. Because patch-type proportions on landscape A change only slightly to create landscapes B and C with one and then two additional patch types, there should be a small decrease in contagion from landscape A to B and then from B to C. Table 1 lists the breakdown of category proportions on the three landscapes and gives the index values computed on these landscapes. The relative contagion indices increase substantially from A to B to C. The relativized indices

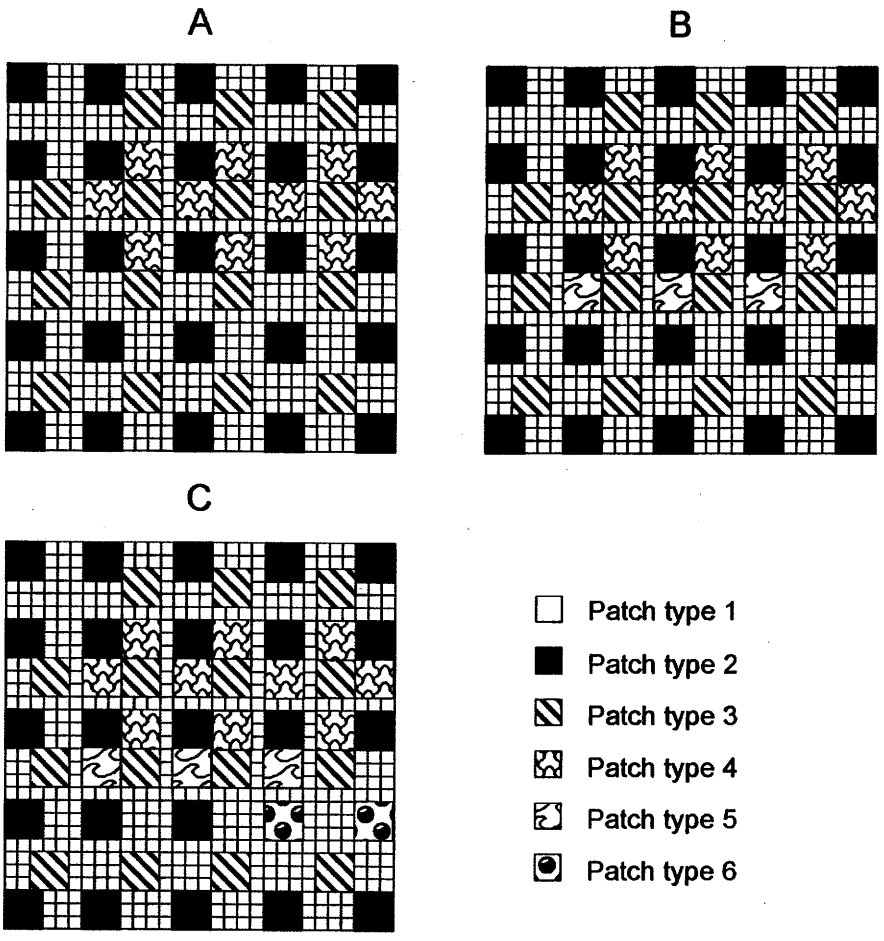

FIGURE 2. Three uniform landscapes; (A) has four patch types, (B) has five patch types, and (C) has six patch types.

are not reflecting changes in contagion, but rather, they are reflecting changes in evenness, as shown by RE.

3.2.3. *Increasing gradient of evenness.* The inappropriateness of using $EE_{\max}$ in an index of contagion is not restricted to the form of ratios. Let us examine the approach used by O'Neill et al. [1988]. They proposed an index using $EE_{\max}$ as an additive term (see equation (1)), though they incorrectly specified $EE_{\max}$. Li and Reynolds [1993]

TABLE 1. Illustrative example showing illogical behavior of relative contagion indices.

	Patch type						Index					
Landscape	1	2	3	4	5	6	RE	RC_1	RC_2	$RC_{\text{unordered}}$	Γ_1	Γ_2
	Proportion						Value					
A	0.50	0.25	0.15	0.10			0.77	0.26	0.20	0.21	0.31	−2.22
B	0.47	0.25	0.15	0.10	0.03		0.71	0.31	0.25	0.27	0.28	−2.41
C	0.47	0.23	0.15	0.10	0.03	0.02	0.66	0.41	0.30	0.32	0.27	−2.51

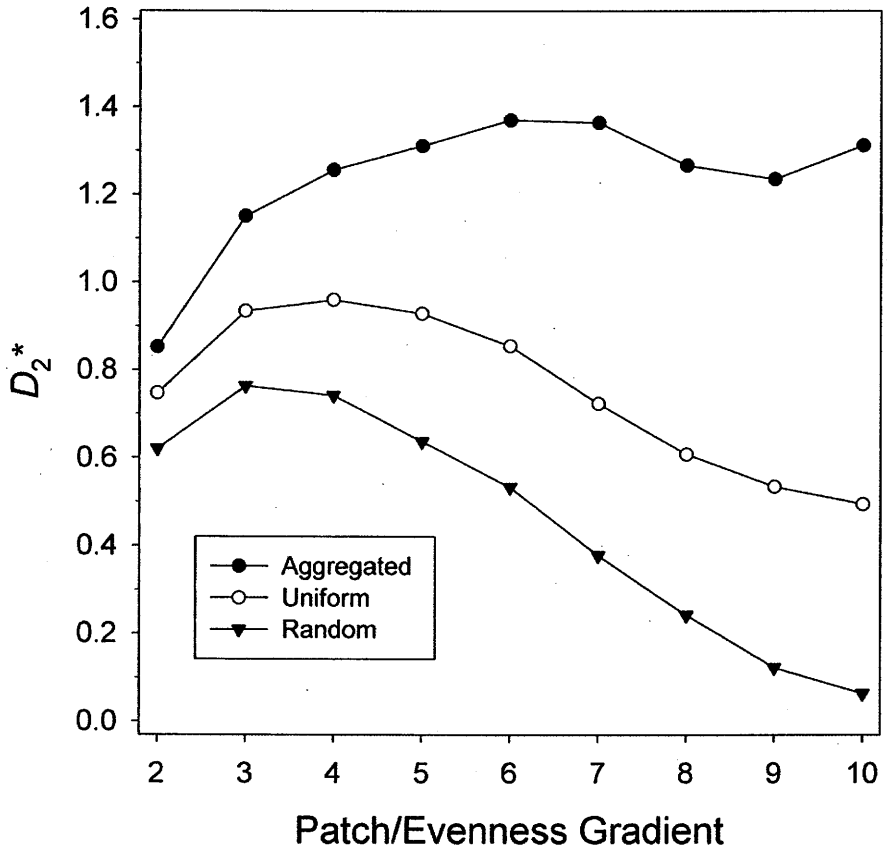

FIGURE 3. Trend lines showing the relationship between D_2^* and the two controlled variables: spatial pattern and number of patch types. There is an increasing gradient of evenness along the x-axis.

derived $EE_{\max} = 2\ln(n)$, therefore the corrected formula for D_2 is

$$D_2^* = 2\ln(n) + \sum_{i=1}^{n}\sum_{j=1}^{n} p_{ij}\ln(p_{ij}), \tag{7}$$

which is the same as equation (1) but with the correct $EE_{\max}$ term. This index, of course, is bounded by 0 and $2\ln(n)$. I computed D_2^* on the simulated landscapes with the progressively increasing gradient of evenness. A graph of these 27 values is presented in Figure 3. Illogical behavior is very apparent, with the lines increasing and then

decreasing. The pattern is contrary to theoretical response, in which each line should monotonically decrease. The lesson is that contagion indices, if they are to retain meaning, should not be relativized.

3.2.4. *The effect of scaling.* From Figures 1 and 3 and Table 1, we can readily see that the effect of scaling contagion relative to the maximum contagion possible creates indices with mathematically undesirable qualities. Such indices are overly sensitive to small variation in composition. Sampling error could easily sway the result one direction or the other, so if contagion indices are to be meaningful they should be relatively insensitive to such a change. This revelation is not new. Sheldon [1969] and Peet [1975] argued against relativizing species diversity indices, and they demonstrated that such indices are mathematically untenable.

4. New contagion indices. One can view the adjacency of patch type i and j as a general problem in waiting times (Feller [1968]) for the encounter of state ij, which follows a geometric distribution. It will be shown that by defining contagion as a generalized function and inserting expected values of random variables based on the encounter of state ij, new and logical indices result.

4.1. Contagion generalized. In a *contagious* landscape, as described by O'Neill et al. [1988] and Riitters et al. [1996], the typical patch type is relatively concentrated. Therefore contagion can be viewed as a function of concentration. Denoting the concentration function of p_{ij} as $C(p_{ij})$, a generalized measure of theoretical contagion on landscape L is given by

$$\Gamma(L) = \phi - \sum\sum p_{ij}C(p_{ij}), \tag{8}$$

where Γ is the contagion index associated with the measure of concentration C, ϕ is any real constant, and $p_{ij} = p_i \cdot p_{j/i}$ (proportion of patch type i times the conditional probability). Because the meaning of contagion is the inverse of the meaning of species diversity, it is necessary to subtract the quantity $\sum\sum p_{ij}C(p_{ij})$ from some constant ϕ to reverse the scale and provide a contagion formulation. Li and Reynolds

[1993] used $\phi = 1$ in formulating relative contagion, defined by equation (2). This caused their indices RC_1 and RC_2 to have the range 0 to 1. The parameter ϕ can be considered a location parameter.

4.2. Geometric distribution. Recall that p_{ij} is the probability that two randomly chosen adjacent pixels belong to type i and j of n patch types. Define $X + 1$ as the number of random picks of adjacent pixels up to and including the first encounter of state ij. This scheme is a general problem in waiting times. Under this scheme X has a geometric distribution:

$$P(X = x|p_{ij}) = p_{ij}(1 - p_{ij})^x, \quad x = 0, 1, 2, \ldots \tag{9}$$

If patch type i (or j) dominates a landscape, for $i \neq j$, a large value of X would be expected. The ratio $X/(X + 1)$ provides a reasonable measure of concentration, varying from 0.5 (low concentration) to 1 (high concentration). For the situation $i = j$, the ratio $X/(X + 1)$ still provides a reasonable measure of concentration, the meaning is simply reversed. That is, if patch type i dominates the landscape, a small value of X would be expected. Now the ratio $X/(X + 1)$ is a random variable, and the average of such a ratio can be constructed in a number of ways; each gives rise to a different index.

4.3. The new indices Γ_1 and Γ_2. Let us assume that $C(p_{ij})$ is represented by $C(p_{ij}) = E[X/(X + 1)|p_{ij}]$. Because $E[X/(X + 1)|p_{ij}] = 1 + p_{ij} \ln(p_{ij})/(1 - p_{ij})$ (see Appendix A for derivations), using this result in equation (8) with $\phi = 1$ and simplifying gives

$$\Gamma_1 = \sum_{i=1}^{n} \sum_{j=1}^{n} \frac{p_{ij}^2 \ln(p_{ij})}{p_{ij} - 1}. \tag{10}$$

This index is bounded between 0 and 1. For a proof see Appendix B.

Let us assume that $C(p_{ij})$ is represented by $C(p_{ij}) = E[X|p_{ij}] \times E[1/(X + 1)|p_{ij}]$. Because $E[X|p_{ij}] = (1 - p_{ij})/p_{ij}$ and $E[1/(X + 1)|p_{ij}] = -p_{ij} \ln(p_{ij})/(1 - p_{ij})$ (see Appendix A for derivations), $C(p_{ij}) = -\ln(p_{ij})$. Use of this result in equation (8) with $\phi = 0$

gives

$$\Gamma_2 = \sum_{i=1}^{n} \sum_{j=1}^{n} p_{ij} \ln(p_{ij}). \tag{11}$$

The quantity $\sum\sum p_{ij} \ln(p_{ij})$ is the entropy information value (Shannon and Weaver [1949]). It has already been established that by defining p_{ij} as the product $p_i \cdot p_{j/i}$, $EE_{\max}$ is $2\ln(n)$ (see equation (4)). Therefore Γ_2 is bounded between $-2\ln(n)$ and 0. The index RC_2 is readily obtained from Γ_2 by dividing by $EE_{\max}$ and adding 1, thus RC_2 is Γ_2 scaled to the interval [0,1].

4.4. Behavior of Γ_1 and Γ_2

4.4.1. *Increasing gradient of evenness.* A graph of the Γ_1 values computed on the simulated landscapes generated with an increasing gradient of evenness is displayed as Figure 4. As is readily seen in Figure 4, Γ_1 is sensitive to both composition and configuration. The three spatial configurations separate out logically with aggregated landscapes having the highest values, followed by uniform landscapes, and then the randomly arranged landscapes having the lowest values. This is expected because random landscapes have little spatial autocorrelation whereas uniform and aggregated landscapes have increasing spatial autocorrelation of patches. There is a sharp decrease in all three curves with increasing number of patches and evenness, covering nearly the full range of index values. This meets with the conceptual definition of contagion. Contrast this with the behavior of D_2^* on the same landscapes (Figure 3). The index D_2^* failed to give monotonically decreasing lines.

A graph of the Γ_2 values computed on these landscapes is displayed as Figure 5. The index Γ_2 shows sensitivity to composition and configuration for these data. The three spatial configurations separate out logically with aggregated landscapes having the highest values, followed by uniform landscapes, and then the randomly arranged landscapes having the lowest values. The lines have less curvature than in

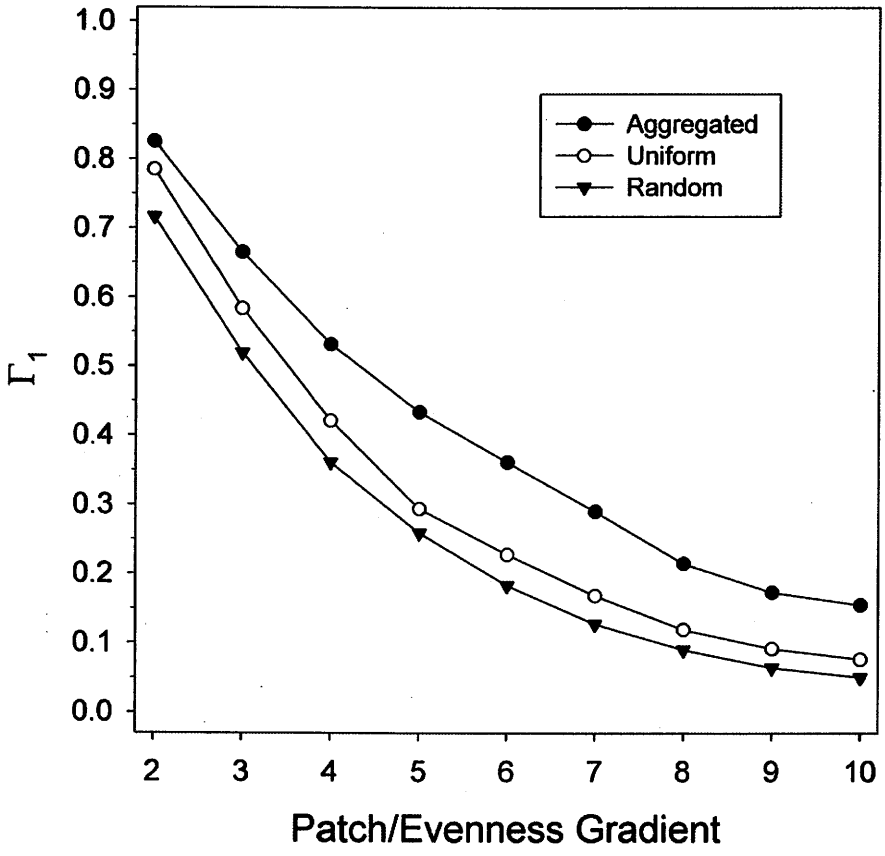

FIGURE 4. Trend lines showing the relationship between Γ_1 and the two controlled variables: spatial pattern and number of patch types. There is an increasing gradient of evenness along the x-axis.

Figure 4 giving slightly better separation among index values at the higher patch/evenness gradient values.

4.4.2. *Same degree of evenness.* A graph of the Γ_1 values from the 27 landscapes with $RE \approx 1$ is displayed as Figure 6. Again we see that Γ_1 distinguishes between the three spatial configurations and decreases with increases in number of land-cover categories. Its behavior is consistent with changes in composition and configuration. Contrast this with the behavior of RC_2 on the same landscapes (Figure 1). The index RC_2 failed to be sensitive to changing composition.

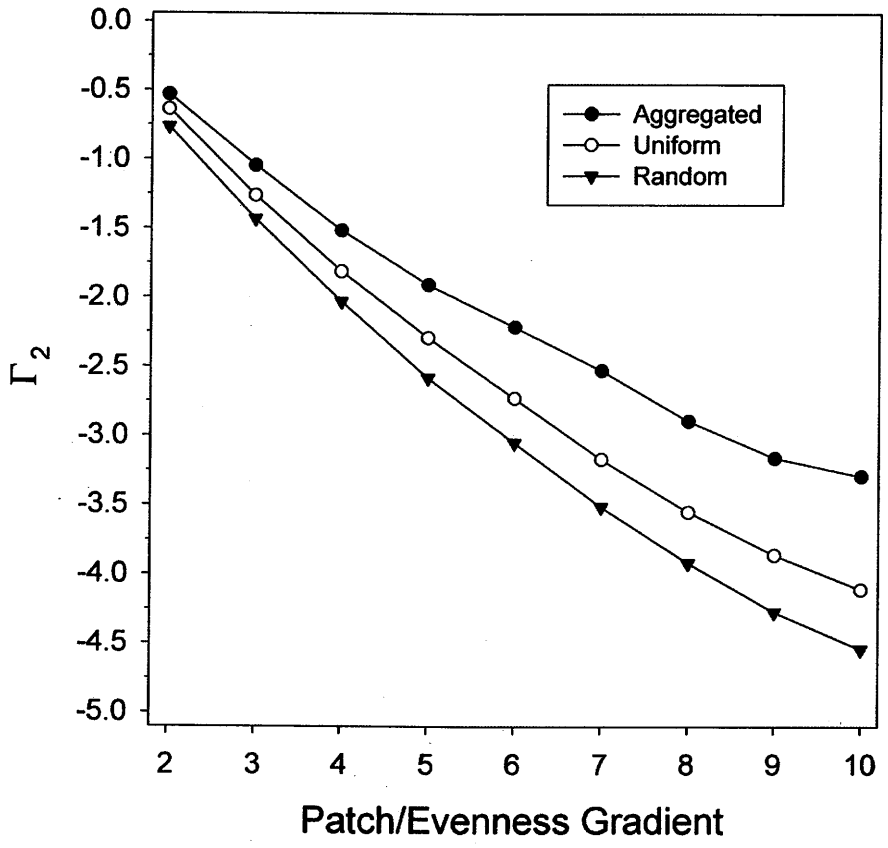

FIGURE 5. Trend lines showing the relationship between Γ_2 and the two controlled variables: spatial pattern and number of patch types. There is an increasing gradient of evenness along the x-axis.

Figure 7 displays a graph of the Γ_2 values computed on these landscapes. Similar to Γ_1, Γ_2 distinguishes among the three spatial configurations and decreases with increases in number of land-cover categories. The lines in Figure 7 have less curvature than in Figure 6, hence they flatten out less, giving slightly better separation between index values at the higher number of patch types.

4.4.3. *Uniform landscapes—disparate evenness.* As a final check on the properties of Γ_1 and Γ_2, let us apply them to the three uniform landscapes of Figure 2. Recall that all of the relative contagion indices failed this test. The computed values of Γ_1 and Γ_2 on these landscapes

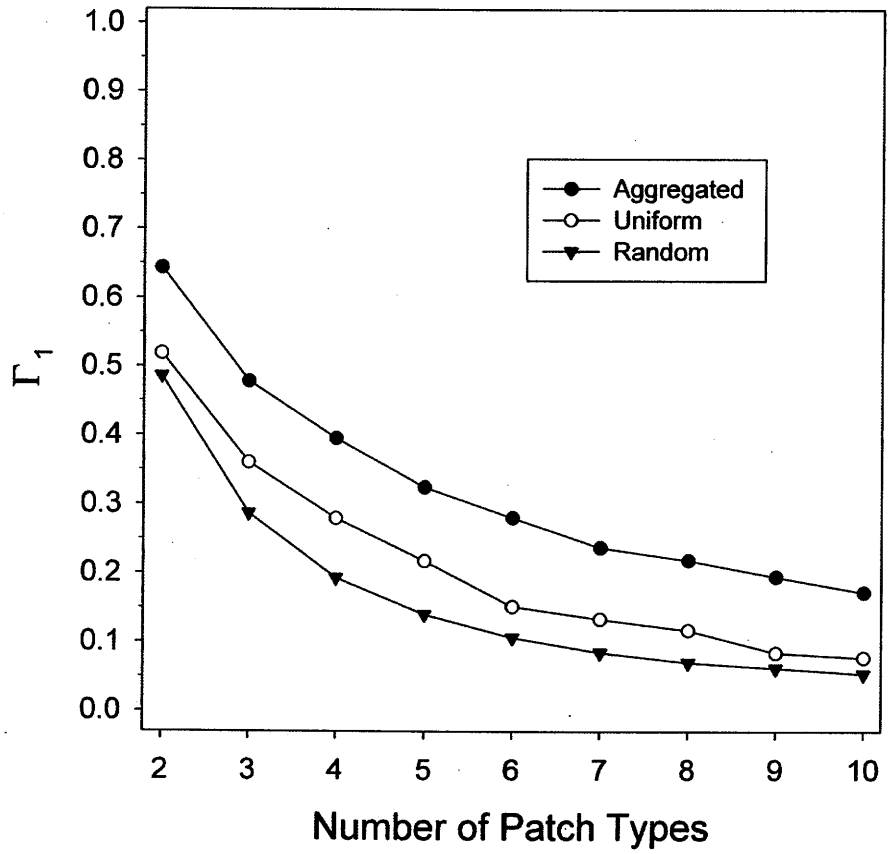

FIGURE 6. Trend lines showing the relationship between Γ_1 and the two controlled variables: spatial pattern and number of patch types. Relative evenness ≈ 1 at each point along the x-axis.

are given in Table 1, and as shown in the table, both indices decrease slightly from landscape A to B to C, as expected from a theoretical measure of contagion.

5. Sampling properties of Γ_1 and Γ_2. In this section, let Γ simultaneously represent Γ_1 and Γ_2. To obtain an estimate of the contagion

$$\Gamma\left(p_{11}, p_{12}, \ldots, p_{nn}\right) \tag{12}$$

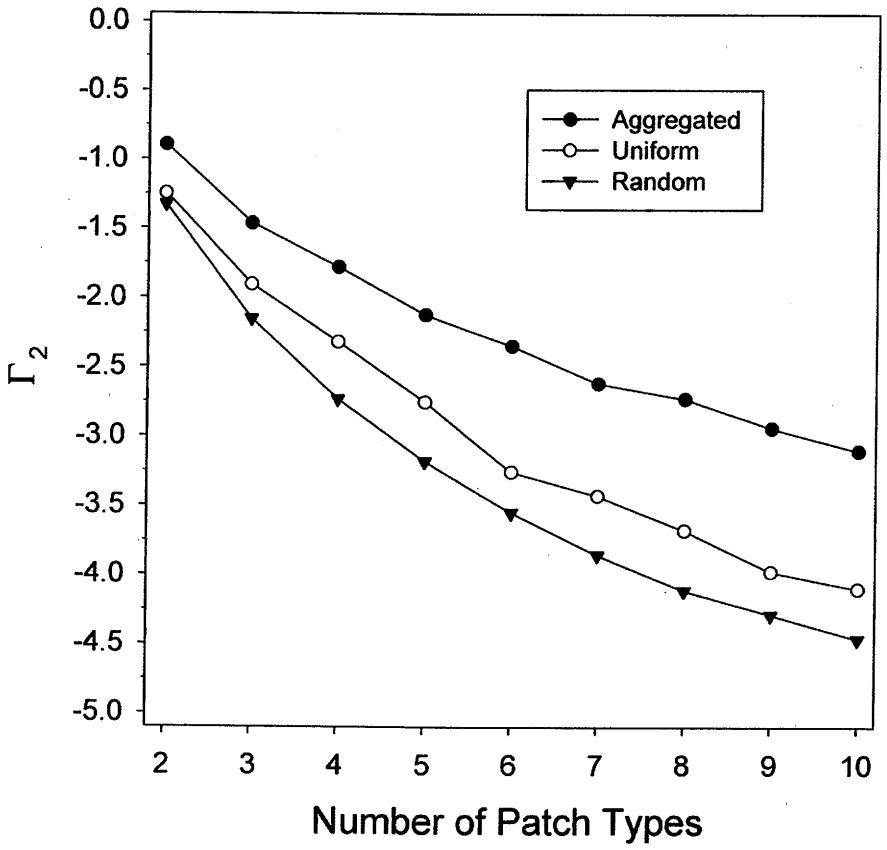

FIGURE 7. Trend lines showing the relationship between Γ_2 and the two controlled variables: spatial pattern and number of patch types. Relative evenness ≈ 1 at each point along the x-axis.

on the basis of a given sampling lattice, the unknown *a priori* probabilities, the p_{ij}s in equation (12) are replaced by estimated $\hat{p}_{ij}$s. In this connection, then, the properties of the random variable

$$\hat{\Gamma} = \Gamma(\hat{p}_{11}, \hat{p}_{12}, \ldots, \hat{p}_{nn}) \tag{13}$$

are what we wish to determine.

5.1. Bias. To estimate the first moment of (13), it is necessary to expand the function in a Taylor series about the point $(p_{11}, \ldots, p_{nn})$

and take the expected value. We can write the expansion as follows:

$$\begin{aligned}(14)\quad \Gamma(\hat{p}_{11},\ldots,\hat{p}_{nn}) &= \Gamma(p_{11},\ldots,p_{nn}) + \sum\sum \Gamma'(p_{ij})(\hat{p}_{ij}-p_{ij}) \\ &+ \frac{1}{2}\sum\sum \Gamma''(p_{ij})(\hat{p}_{ij}-p_{ij})^2 + \frac{1}{6}\sum\sum \Gamma'''(p_{ij})(\hat{p}_{ij}-p_{ij})^3 \\ &+ \frac{1}{24}\sum\sum \Gamma^{(4)}(p_{ij})(\hat{p}_{ij}-p_{ij})^4 + \cdots\end{aligned}$$

The expectation of $\Gamma(\hat{p}_{11},\ldots,\hat{p}_{nn})$ involves the central moments of the random variables $\hat{p}_{ij}$ $(i, j = 1,\ldots, n)$. The multinomial distribution arises in categorical data analysis. The genesis of the multinomial distribution stems from T independent trials, where each trial can result in only one of n mutually exclusive events. See Ratnaparkhi [1985] for background on the multinomial distribution. Let T be the total number of lattice plots, and let $\varepsilon_{ij} = \hat{p}_{ij} - p_{ij}$. For the multinomial distribution, the moment-generating function is (Shenton and Hutcheson [1969]):

$$(15)\qquad E\left[e^{\alpha\varepsilon_{ij}}\right] = \left(E\left[e^{\alpha(x_{ij}/T - p_{ij}/T)}\right]\right)^T,$$

where x_{ij} takes the value 1 with probability p_{ij}, and 0 with probability $q_{ij} = 1 - p_{ij}$. Using equation (15), the following values are obtained:

$$\begin{aligned}(16)\qquad & E[\varepsilon_{ij}] = 0, \quad E\left[\varepsilon_{ij}^2\right] = p_{ij}(1-p_{ij})/T, \\ & E\left[\varepsilon_{ij}^3\right] = \left(2p_{ij}^3 - 3p_{ij}^2 + p_{ij}\right)/T^2, \\ & E\left[\varepsilon_{ij}^4\right] = O(T^{-2}), \quad E\left[\varepsilon_{ij}^5\right] = O(T^{-3}).\end{aligned}$$

By substituting the appropriate expressions from (16) into (14) and simplifying, we obtain the first moment or mean of the random variable $\hat{\Gamma}$:

$$\begin{aligned}(17)\quad E[\hat{\Gamma}] &= \Gamma(p_{11},\ldots,p_{nn}) + o(T^{-1}) + o(T^{-2}) + o(T^{-3}) + \cdots \\ &= \Gamma + o(T^{-1}).\end{aligned}$$

From (17), we can deduce that $\hat{\Gamma}_1$ and $\hat{\Gamma}_2$ are biased, but for any reasonable size T the bias is very small, and in fact is less than T^{-1}.

5.2. Variance. The estimated $\hat{\Gamma}$ equals the true Γ plus a random error ξ, i.e., $\hat{\Gamma} = \Gamma + \xi$. By definition, $E[\xi^2] = E[(\hat{\Gamma} - \Gamma)^2]$, and the variance of $\hat{\Gamma}$ is $E[\xi^2] - E^2[\xi]$. From (17), we know that $E[\xi] = o(T^{-1})$, consequently $E^2[\xi] = o(T^{-2})$, which for practical purposes is negligible. Therefore, the variance of $\hat{\Gamma}$ is:

$$\text{var}(\hat{\Gamma}) = E[\xi^2] = E[(\hat{\Gamma} - \Gamma)^2]. \tag{18}$$

A common approach for establishing the variance of a scalar statistic that is a function of many variables is the delta method (Rao [1965, pp. 321–322], Bishop et al. [1975, pp. 492–497]). The delta method uses the first-order multivariate Taylor series expansion to produce an estimated variance, i.e., $\widehat{\text{var}}(\hat{\Gamma})$. The variance derivations for $\hat{\Gamma}_1$ and $\hat{\Gamma}_2$ are given in Appendix C. For $\hat{\Gamma}_1$ we have

$$\widehat{\text{var}}(\hat{\Gamma}) \approx \frac{1}{T}\left\{\sum_{i=1}^{n}\sum_{j=1}^{n}\hat{p}_{ij}\frac{\left[\hat{p}_{ij}^2(1+\ln(\hat{p}_{ij})) - \hat{p}_{ij}(1+2\ln(\hat{p}_{ij}))\right]^2}{(\hat{p}_{ij}-1)^4} - \left[\sum_{i=1}^{n}\sum_{j=1}^{n}\frac{\hat{p}_{ij}^3(1+\ln(\hat{p}_{ij})) - \hat{p}_{ij}^2(1+2\ln(\hat{p}_{ij}))}{(\hat{p}_{ij}-1)^2}\right]^2\right\}. \tag{19}$$

For $\hat{\Gamma}_2$ the estimated variance is[3]

$$\widehat{\text{var}}\left(\hat{\Gamma}_2\right) \approx \frac{\sum_{i=1}^{n}\sum_{j=1}^{n}\hat{p}_{ij}\ln^2(\hat{p}_{ij}) - \left[\sum_{i=1}^{n}\sum_{j=1}^{n}\hat{p}_{ij}\ln(\hat{p}_{ij})\right]^2}{T}. \tag{20}$$

5.3. Consistency. The property of consistency ensures that an estimate is close to the true parameter value with a high probability if the sample size is sufficiently large. Let $\hat{\theta}_T$ be an estimator of θ based on a sample of size T. Sufficient conditions for an estimator $\hat{\theta}_T$ to be consistent for θ are (Judge et al. [1988, p. 85]):

$$\lim_{T\to\infty} E[\hat{\theta}_T] = 0 \tag{21a}$$

$$\lim_{T\to\infty} \operatorname{var}(\hat{\theta}_T) = 0. \tag{21b}$$

An estimator that satisfies (21a) is said to be asymptotically unbiased. Thus an estimator is consistent if any bias it has goes to zero as the sample size increases and if its variance goes to zero as $T \to \infty$. The limit of equation (17) is Γ so condition (21a) is met; and the limit of equations (19) and (20) is zero so condition (21b) is met. Thus $\hat{\Gamma}_1$ and $\hat{\Gamma}_2$ are consistent estimators.

5.4. Asymptotic distribution. Kempthorne and Folks [1971, pp. 112–115 and pp. 120–121] have shown how the probabilities for the multinomial distribution tend with increasing sample size to the ordinates for the multivariate normal distribution. They used a moment-generating function argument to show that the limiting distribution of the multinomial is the multivariate normal distribution. Because $\hat{\Gamma}_1$ and $\hat{\Gamma}_2$ are functions of multinomial probabilities, the k-variate normal condition of equation (13) is met, thus proving asymptotic normality for $\hat{\Gamma}_1$ and $\hat{\Gamma}_2$.

6. Application: Analysis of contagion on three physiographic provinces in Alabama. Much public attention has been given to growth declines of southern commercial forests (Sheffield et al. [1985], Zeide [1992]). Survey units in Alabama showed a pattern that created the suspicion that widespread growth declines might be occurring in Alabama. Thomas and Parresol [1989] were able to show, using Simpson's paradox, that basal area growth was (i) consistent with changes in tree frequency in diameter classes and (ii) relatively constant over the most recent inventories. Simple comparison of radial growth was misleading. A look at landscape diversity is of interest in this region, especially for broad-scale management considerations. Physiographic provinces for Alabama are given by Hodgkins et al. [1979] (Figure 8).

6.1. Study areas and data. Three adjacent physiographic provinces in Alabama were chosen for study: (i) Great Appalachian Valley Province, (ii) Blue Ridge-Talladega Mountain Province, and

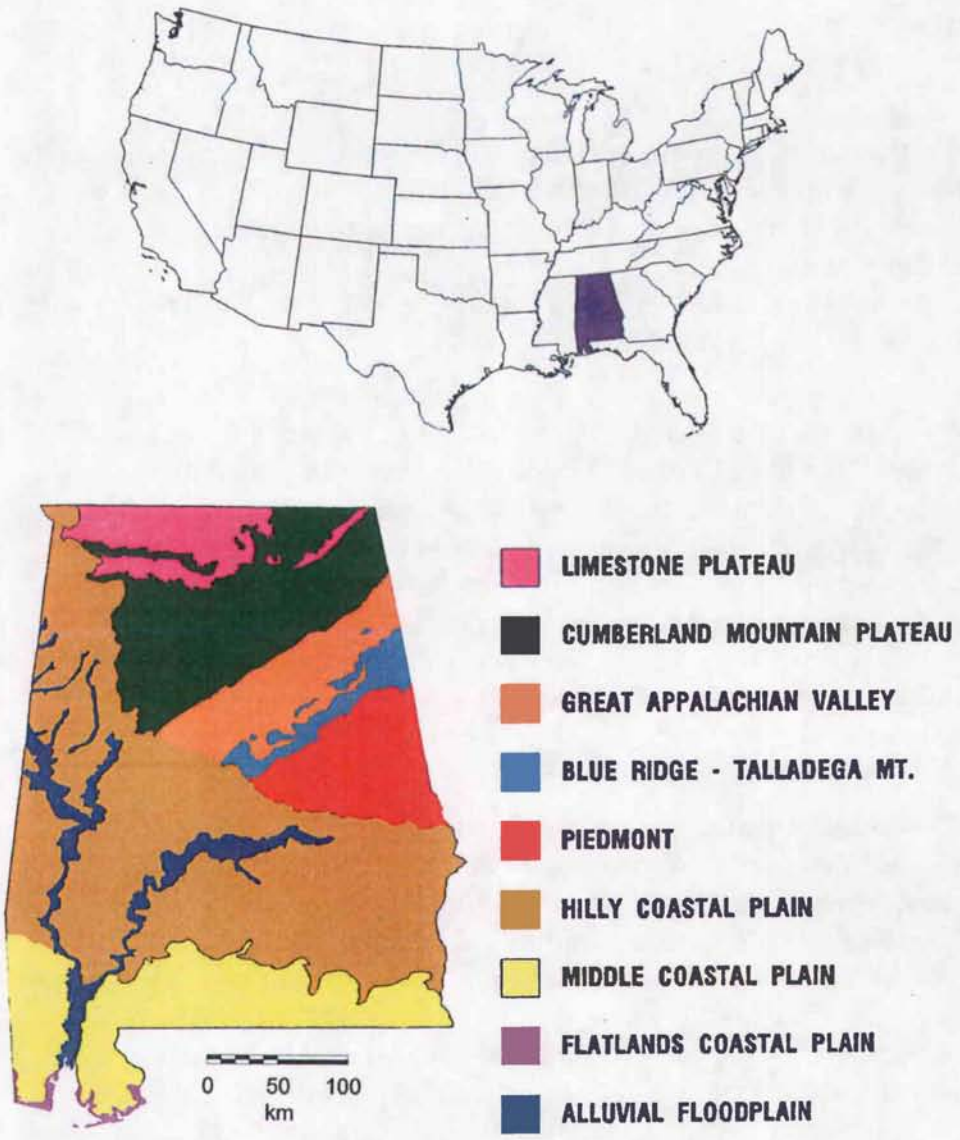

FIGURE 8. The nine physiographic provinces of Alabama.

(iii) Piedmont Province (see Figure 8). FIA forest cover type data for these provinces were obtained from the national FIA website (http://www.fia.fs.fed.us).[4] General forest cover types are listed in Table 2. Each physiographic province point coverage was apportioned into

TABLE 2. USDA Forest Service general forest cover types[a] occurring on three physiographic provinces in the state of Alabama, USA.

General forest cover types	Species
Longleaf-slash pine	*Pinus palustris-Pinus elliottii*
Loblolly-shortleaf pine	*Pinus taeda-Pinus echinata*
Oak-pine	*Quercus* sp.-*Pinus* sp.
Oak-hickory	*Quercus* sp.-*Carya* sp.
Oak-gum-cypress	*Quercus* sp.-*Liquidambar styraciflua-Taxodium distichum*
Elm-ash-cottonwood	*Ulmus* sp.-*Fraxinus* sp.-*Populus* sp.
Nontyped	
Nonforest	

[a]Source: May [1990, p. 6].

Thiessen polygons, and polygons of the same forest cover type were marked the same to create a landscape-level view of cover types for each province for the survey years 1972, 1982, and 1990 (Figure 9). Proportions of each cover type on each province by survey year are given in Table 3.

6.2. Hypotheses and hypothesis testing. It is generally believed that prior to the 1900s forested landscapes in the South were more homogeneous and contiguous than today. Exploitative logging, agriculture, forest-type conversion, and other factors have altered, and continue to alter, the mosaic of forest cover types on the landscape. Today landscape flux (changes in composition and/or configuration) can possibly occur on the time scale of a decade. Therefore, it is natural to hypothesize that landscape flux is occurring on the physiographic provinces. Also, it is of general interest to compare physiographic provinces for similarity or differences in contagion. Using the new indices, contagion values (C) were computed for each province for the three survey periods. Let A represent the Great Appalacian Valley Province, let B represent the Blue Ridge-Talladega Mountain Province,

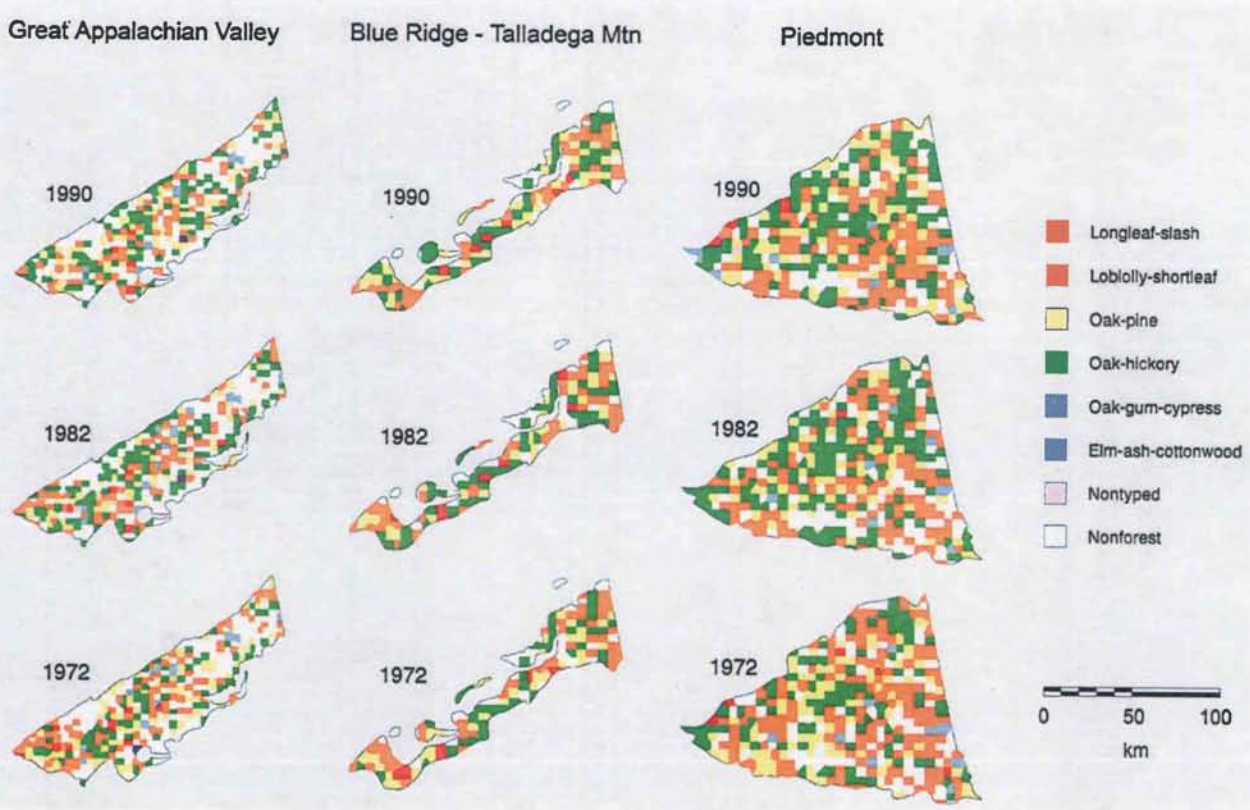

FIGURE 9. Forest cover type changes through time in the Great Appalachian Valley, Blue Ridge-Talladega Mountain, and Piedmont physiographic provinces based on Southern Forest Inventory and Analysis survey data.

TABLE 3. Proportion of each forest cover type on each province by survey year.

Forest cover type	Great Appalachian Valley			Blue Ridge – Talladega Mt.			Piedmont		
	72	82	90	72	82	90	72	82	90
	Values in percent								
Longleaf-slash pine	2.2	1.5	1.0	3.9	4.5	4.5	1.2	0.2	0.7
Loblolly-shortleaf pine	22.4	18.9	18.2	26.5	24.5	22.6	34.5	26.4	27.4
Oak-pine	19.2	12.5	15.5	23.9	18.7	23.9	20.0	15.6	18.8
Oak-hickory	16.7	26.3	24.8	24.5	31.0	27.7	21.8	33.3	32.0
Oak-gum-cypress	2.9	3.2	2.0		0.6		2.2	1.7	1.7
Elm-ash-cottonwood	0.2	0.2	0.2						
Nontyped		0.2							0.2
Nonforest	36.4	37.1	38.3	21.3	20.6	21.3	20.3	22.7	19.1

and let P represent the Piedmont Province. The following constitute a logical set of hypotheses for the landscape data:

1. For Appalachian, H_0: $C_{72} = C_{82} = C_{90}$
2. For Blue Ridge, H_0: $C_{72} = C_{82} = C_{90}$
3. For Piedmont, H_0: $C_{72} = C_{82} = C_{90}$
4. For 1972, H_0: $C_A = C_B = C_P$
5. For 1982, H_0: $C_A = C_B = C_P$
6. For 1990, H_0: $C_A = C_B = C_P$.

Variance formulas have been derived for the two new indices, and the distribution of both indices is asymptotically normal, hence hypothesis testing can be accomplished through application of one-way analysis of variance (ANOVA). The tests of hypotheses were conducted using $\alpha = .10$. This level was chosen to increase power of the test. The results of the hypothesis tests were used to draw general conclusions about forest cover type diversity on the three physiographic provinces and use of the new indices.

7. Results and discussion. Table 4 lists the $\hat{\Gamma}_1$ values and their corresponding variances computed on each of the provinces at the three survey periods. All $\hat{\Gamma}_1$ values in Table 4 are fairly low, reflecting the fact that all three landscapes have many patches. Compositional change, in terms of changing proportions of forest cover types (see Table 3), is probably more responsible for the slight differences in $\hat{\Gamma}_1$ values than configuration. From the tests of hypotheses in Table 4, we can see that there was a significant increase in contagion in the Great Appalachian Valley in 1990 over the other two provinces. All in all there is great uniformity in contagion values in Table 4 indicating there has been little or no change in processes affecting contagion over the two decades and that all three provinces operate under the same influences.

The $\hat{\Gamma}_2$ contagion values and their corresponding variances computed on each of the provinces at the three survey periods are listed in Table 5. This table tells much the same story as Table 4, but there are some interesting differences. The first hypothesis test in Table 5 indicates that contagion has increased significantly in the Great Appalachian Valley in 1990 over the previous two periods. The fourth hypothesis test

TABLE 4. Contagion values, variances, and F-tests using $\hat{\Gamma}_1$ on three physiographic provinces in Alabama during three survey periods.

Province	Year	$\hat{\Gamma}_1$	$\widehat{\text{var}}(\hat{\Gamma}_1)$	T
Great Appalachian Valley	1972	0.1713	0.00003415	407
Great Appalachian Valley	1982	0.1798	0.00004075	407
Great Appalachian Valley	1990	0.1888	0.00003319	407
Blue Ridge-Talladega Mt.	1972	0.1736	0.00004874	155
Blue Ridge-Talladega Mt.	1982	0.1725	0.00005597	155
Blue Ridge-Talladega Mt.	1990	0.1709	0.00005583	155
Piedmont	1972	0.1778	0.00002236	409
Piedmont	1982	0.1864	0.00001777	409
Piedmont	1990	0.1787	0.00001766	409

For Appalachian, H_0: $\Gamma_{72} = \Gamma_{82} = \Gamma_{90}$; $F = 2.128$, $p = 0.120$.
For Blue Ridge, H_0: $\Gamma_{72} = \Gamma_{82} = \Gamma_{90}$; $F = 0.035$, $p = 0.965$.
For Piedmont, H_0: $\Gamma_{72} = \Gamma_{82} = \Gamma_{90}$; $F = 1.154$, $p = 0.316$.
For 1972, H_0: $\Gamma_A = \Gamma_B = \Gamma_P$; $F = 0.349$, $p = 0.706$.
For 1982, H_0: $\Gamma_A = \Gamma_B = \Gamma_P$; $F = 1.599$, $p = 0.203$.
For 1990, H_0: $\Gamma_A = \Gamma_B = \Gamma_P$; $F = 2.926$, $p = 0.054$.
Note: In the table footnotes, the subscript A stands for the Great Appalachian Valley, B is for the Blue Ridge-Talladega Mountain, and P is for the Piedmont.

tells us that contagion is lower in the Great Appalachian Valley than in the other two provinces in 1972. The fifth hypothesis test indicates that contagion is higher in the Piedmont Province than in the other two provinces in 1982. Hence there were three significant tests using $\hat{\Gamma}_2$ whereas there was only one significant test using $\hat{\Gamma}_1$. From this, we can conclude that use of $\hat{\Gamma}_1$ provides a more conservative test. Let us examine composition and configuration on the landscapes to try to understand the significant tests.

7.1. Composition. From Table 3, it is apparent that the longleaf-slash, oak-gum-cypress, and elm-ash-cottonwood types are minor components of the provinces. Proportions range from less than 1% for the elm-ash-cottonwood type in the Great Appalachian Valley Province to about 5% for longleaf-slash in the Blue Ridge-Talladega Mountain

TABLE 5. Contagion values, variances, and F-tests using $\hat{\Gamma}_2$ on three physiographic provinces in Alabama during three survey periods.

Province	Year	$\hat{\Gamma}_2$	$\widehat{\text{var}}(\hat{\Gamma}_2)$	T
Great Appalachian Valley	1972	−3.0609	0.001819	407
Great Appalachian Valley	1982	−3.0167	0.002158	407
Great Appalachian Valley	1990	−2.9075	0.001815	407
Blue Ridge-Talladega Mt.	1972	−2.9513	0.002264	155
Blue Ridge-Talladega Mt.	1982	−2.9813	0.002895	155
Blue Ridge-Talladega Mt.	1990	−2.9747	0.002111	155
Piedmont	1972	−2.9517	0.001325	409
Piedmont	1982	−2.8583	0.001088	409
Piedmont	1990	−2.9340	0.001286	409

For Appalachian, H_0: $\Gamma_{72} = \Gamma_{82} = \Gamma_{90}$; $F = 3.231$, $p = 0.040$.
For Blue Ridge, H_0: $\Gamma_{72} = \Gamma_{82} = \Gamma_{90}$; $F = 0.102$, $p = 0.903$.
For Piedmont, H_0: $\Gamma_{72} = \Gamma_{82} = \Gamma_{90}$; $F = 1.997$, $p = 0.136$.
For 1972, H_0: $\Gamma_A = \Gamma_B = \Gamma_P$; $F = 2.451$, $p = 0.087$.
For 1982, H_0: $\Gamma_A = \Gamma_B = \Gamma_P$; $F = 3.839$, $p = 0.022$.
For 1990, H_0: $\Gamma_A = \Gamma_B = \Gamma_P$; $F = 0.779$, $p = 0.459$.
Note: In table footnotes, the subscript A stands for the Great Appalachian Valley, B is for the Blue Ridge-Talladega Mountain, and P is for the Piedmont.

Province. Though minor, these forest types nonetheless play a role in determining the contagion of the provinces.

Again referring to Table 3, there has been a 4–7% decrease in the loblolly-shortleaf type from 1972 to 1990 in the three provinces. The oak-pine type has declined by 4% in the Great Appalachian Valley; it declined by 5% in 1982 but regained the lost 5% in 1990 in the Blue Ridge-Talladega Mountain Province; and it declined nearly 5% in 1982 but regained 3% in 1990 on the Piedmont Province. The oak-hickory type has increased notably in the Great Appalachian Valley (8%) and the Piedmont (11%) Provinces between 1972 and 1990, and was up 7% in 1982 but lost 4% in 1990 in the Blue Ridge-Talladega Mountain Province. The nonforest proportion has been relatively stable, shifting only 1% to 3.5% in the provinces between survey periods. It is worth noting that the Great Appalachian Valley Province has considerably

more nonforest area, about 36% to 38%, compared to the other two provinces, which have around 19–23% nonforest area.

7.2. Configuration. The landscape-level views of forest cover types in Figure 9 reveal subtle rather than dramatic changes in pattern and composition occurring in the provinces between 1972 and 1990. For the three physiographic provinces, the pattern appears to be a mix of random and clumped. Obviously, all provinces display a degree of fragmentation. Fragmentation at this geographic level results from a complex mix of cities and towns, dams and artificial lakes, forest type conversion, farming, and inherent site conditions such as topography, soil type, and moisture.

The Great Appalachian Valley Province has a topography of folded mountain ridges with interspersed valleys and hills. The mountain ridges are oriented from southwest to northeast. Under the Great Appalachian Valley section of Figure 9, we can see that the nonforest type occurs in three concentrated clumps. These clumps are the result of two major cities and a man-made lake, with Birmingham in the southwest and Gadsden and Weiss Lake in the northeast. The Coosa River flows through this province coming in from the east. The Coosa was dammed to make Weiss Lake. In this province, the oak-gum-cypress and the elm-ash-cottonwood types occur in the broad valley areas along the Coosa and its tributaries. The ridges and slopes support extensive areas of hardwood forests, and we can see clumping of the oak-hickory type. Pine management, both planted and natural, is important in this region, and we can see some clumping of the loblolly-shortleaf type. The other types are more scattered.

The smallest of the three provinces, the Blue Ridge-Talladega Mountain, is a topographically reduced extension of the heavy slates and quartzites of the western Blue Ridge Mountains of East Tennessee and North Georgia. This province lacks the elm-ash-cottonwod type and the oak-gum-cypress type (except in 1982 where it shows up at a plot near where the Coosa crosses the province). The nonforest areas (see Figure 9) are scattered, but one clump shows up at the northeast neck of the province coinciding with the city of Anniston. Immediately to the west of the "neck" is a narrow cut out area belonging to the Great Appalachian Valley that contains a part of this nonforest city area.

We can see in Figure 9 that this province has some clumping in the loblolly-shortleaf and oak-hickory types that relates to the topography and soil characteristics of the province.

Heading south out of the Blue Ridge-Talladega Mountain Province, we drop in elevation and enter into the Piedmont Province. Cultivation was once widespread in this province. The Tallapoosa River generally runs north to south nearly through the center of the province with a major man-made lake, Lake Martin, formed close to the southern border. In Figure 9 (under the Piedmont section) this lake shows up as a large nonforest block near the southern border a little to the west of center. In the southeast of the province, there is a northeast to southwest line of towns (Lanett and Valley, Opelika, and Auburn) along interstate 85, which show up as three small nonforest blocks. Farming, though not as extensive as in years past, is still important in the region, creating small nonforest fragments across the province. Additionally, we can see in Figure 9 that there is clumping of the loblolly-shortleaf and oak-hickory types in this province.

7.3. Conclusions. From our examination of composition and configuration and the contagion tests, it can generally be concluded that (i) there has been a minor shift in loblolly-shortleaf and oak-pine acreage into oak-hickory acreage; (ii) the overall landscape pattern in the three provinces is similar, being a mix of random and clumped; (iii) the loblolly-shortleaf and oak-hickory forest cover types occur in moderate-to-large clumps while the others occur in small (relative to the landscape) well-intermixed patches; and (iv) there have been only small, though in some cases statistically significant, changes in contagion on the provinces. Both $\hat{\Gamma}_1$ (Table 4, test 6) and $\hat{\Gamma}_2$ (Table 5, test 1) indicate a significant increase in contagion for the Great Appalachian Valley in 1990. The large proportion of nonforest and clumpiness of this type are probably most responsible for this result. In 1972, contagion appears to be lowest on the Great Appalachian Valley Province (Table 5, test 4). This province has the greater richness, which may account for its lower contagion. Finally, in 1982 the Piedmont has greater contagion over the other two provinces (Table 5, test 5). The Piedmont experienced greater composition changes from 1972 to 1982 than the other provinces, which probably accounts for its greater contagion.

8. Concluding remarks. Based on the simulations, both Γ_1 and Γ_2 behaved in a manner consistent with the concept of contagion. Both indices were sensitive to changes in composition and configuration and correctly ordered spatial pattern with aggregated > uniform > random. The graph of Γ_1 values displayed more curvature (see Figures 4 and 6) than the graph of Γ_2 values (see Figures 5 and 7). Hence for landscapes having many patch types, Γ_2 may give better separation. A feature of Γ_2 is its negative scale. One could specify a positive constant for ϕ (see equation (8)) and thereby translate the axis to give positive readings, but there is no constant other than $\phi = 0$ that will retain the origin as an end point in the range interval. We have already seen the deleterious effects of specifying a variable value for ϕ such as $2\ln(n)$ in equation (7).

From a theoretical point of view, there is nothing inherently wrong with having a negative scale, but from a practical point of view most users of indices prefer a positive scale. Thus, the index Γ_1 is appealing because of its positive scale. Also, Γ_1 possesses the fixed range (0,1] providing a ready interpretation of no contagion at the lower extreme and perfect contagion at the upper extreme, with degrees of contagion in between. The index Γ_2 has a nonstationary range dependent on the quantity $2\ln(n)$, which adds a layer of complexity in interpreting contagion on the range of Γ_2.

Because Γ_2 has an expanding range with increasing number of patch types, one could raise the issue of what is a meaningful difference. Past a certain point of fragmentation or with increasing evenness and number of categories, Γ_1 tends to flatten out whereas Γ_2 keeps increasing its range and can take on lower and lower values. This author concurs with others such as O'Neill et al. [1988] and Riitters et al. [1996], who want measures of contagion to assess dominance or concentration.[5] Philosophically then, this author believes that below a certain point, differences have little functional significance on the landscape. The "conservativeness" of Γ_1 reflects this philosophical niche. If one does not subscribe to this ideology, then Γ_2 would seem preferable.[6]

A contagion index can be considered as a sum of multinomial probabilities. Using properties of the multinomial distribution in a Taylor series expansion of $\hat{\Gamma}_1$ and $\hat{\Gamma}_2$, the bias of these statistics is shown to be $o(T^{-1})$ where T is total number of observations. Using the delta method, a standard linear approximation formula, variance equations

were derived for $\hat{\Gamma}_1$ and $\hat{\Gamma}_2$. A function of a multivariate normal is itself normally distributed. Because multinomial probabilities have a limiting multivariate normal distribution, $\hat{\Gamma}_1$ and $\hat{\Gamma}_2$ are asymptotically normal.

With the sampling properties worked out, an analysis of forest cover type contagion was conducted on three physiographic provinces in Alabama based on available FIA data. Field-determined forest cover type data are available from the USDA Forest Service-FIA surveys from sampling lattices covering the whole of the United States dating back to the 1930s.

A host of tools are today available to policy makers and forestry practitioners to assess the state of forests and to help guide in their management for sustainability. In dealing with landscapes or regions, GIS and landscape indices are important tools for characterizing and comparing landscape diversity.

Acknowledgments. I wish to thank Dr. Harbin Li for use of his landscape simulation program, SHAPC, and for his valuable comments. I would like to thank Lisa Parresol for her graphics of Figures 8 and 9. I also wish to thank the anonymous referees for their constructive reviews of the manuscript.

APPENDIX A: EXPECTED VALUE CALCULATIONS

The contagion formulas for Γ_1 (equation (10)) and Γ_2 (equation (11)) come from particular expected values based on a geometric random variable (see equation (9)). Let $q_{ij} = (1 - p_{ij})$, the required expected values are:

$$
\begin{aligned}
\text{(A1)} \qquad E[X \mid p_{ij}] &= \sum_{x=0}^{\infty} x p_{ij} q_{ij}^{x} \\
&= p_{ij}q_{ij} + 2p_{ij}q_{ij}^2 + 3p_{ij}q_{ij}^3 + \cdots \\
&= p_{ij}q_{ij}(1 + 2q_{ij} + 3q_{ij}^2 + \cdots) \\
&= p_{ij}q_{ij}(1 - q_{ij})^{-2} = (1 - p_{ij})/p_{ij},
\end{aligned}
$$

$$\text{(A2)} \quad E[1/(X+1)|p_{ij}] = \sum_{x=0}^{\infty} \frac{1}{x+1} p_{ij} q_{ij}^x$$
$$= p_{ij} + {}^1\!/_2 p_{ij} q_{ij} + {}^1\!/_3 p_{ij} q_{ij}^2 + {}^1\!/_4 p_{ij} q_{ij}^3 + \cdots$$
$$= p_{ij}(q_{ij} + {}^1\!/_2 q_{ij}^2 + {}^1\!/_3 q_{ij}^3 + {}^1\!/_4 q_{ij}^4 + \cdots)/q_{ij}$$
$$= p_{ij}[-\ln(1-q_{ij})]/q_{ij}$$
$$= -p_{ij}\ln(p_{ij})/(1-p_{ij}),$$

$$\text{(A3)} \quad E\,[X/(X+1)|p_{ij}] = \sum_{x=0}^{\infty} \frac{x}{x+1} p_{ij} q_{ij}^x$$
$$= {}^1\!/_2 p_{ij} q_{ij} + {}^2\!/_3 p_{ij} q_{ij}^2 + {}^3\!/_4 p_{ij} q_{ij}^3 + \cdots$$
$$= p_{ij}({}^1\!/_2 q_{ij}^2 + {}^2\!/_3 q_{ij}^3 + {}^3\!/_4 q_{ij}^4 + \cdots)/q_{ij}$$
$$= p_{ij}[1/(1-q_{ij}) - 1 + \ln(1-q_{ij})]/q_{ij}$$
$$= 1 + p_{ij}\ln(p_{ij})/(1-p_{ij}).$$

All three expected values involve solutions of infinite series. The series solutions are given below.

One of the most celebrated series in mathematics is the *binomial series* (Salas and Hille [1974, pp. 533–534]):

$$\text{(A4)} \quad \sum_{k=0}^{\infty} (\pm 1)^k \binom{\alpha}{k} x^k = (1 \pm x)^{\alpha}, \quad x^2 < 1,$$

where $\binom{\alpha}{k}$ is the kth binomial coefficient. For the binomial $(1-x)^{-2}$ the following sequence is obtained

$$\text{(A5)} \quad 1 + 2x + 3x^2 + 4x^3 + \cdots$$

which is the same sequence in equation (A1).

To solve the power series embedded in equation (A2), begin by noting that $\frac{d}{dx} - \ln u = -\frac{1}{u}\frac{du}{dx}$. We can sum the power series

$$\text{(A6)} \qquad \sum_{k=1}^{\infty} \frac{x^k}{k} = x + 1/2x^2 + 1/3x^3 + 1/4x^4 + \cdots, \quad x^2 < 1$$

by setting

$$\text{(A7)} \qquad f(x) = \sum_{k=1}^{\infty} \frac{x^k}{k}, \quad x^2 < 1$$

and applying the differentiability of power-series theorem (see Salas and Hille [1974, p. 526]) to obtain

$$\text{(A8)} \qquad f'(x) = \sum_{k=1}^{\infty} \frac{kx^{k-1}}{k} = \sum_{k=1}^{\infty} x^{k-1} = \sum_{k=0}^{\infty} x^k = \frac{1}{1-x},$$

the last sum being the well-known geometric series. Because $f(0) = 0$ and $f'(x) = \frac{1}{1-x}$, we must have

$$\text{(A9)} \qquad f(x) = -\ln(1-x).$$

To solve the power series embedded in equation (A3), we begin by noting the summation formula

$$\text{(A10)} \qquad \sum_{k=1}^{\infty} \frac{k-1}{k} x^k = 1/2x^2 + 2/3x^3 + 3/4x^4 + \cdots$$

We can take (A10) and rearrange it into two series with known values and thereby arrive at the solution.

$$\text{(A11)} \qquad \begin{aligned} \sum_{k=1}^{\infty} (k-1)\frac{x^k}{k} &= \sum_{k=1}^{\infty} x^k - \sum_{k=1}^{\infty} \frac{x^k}{k} \\ &= \frac{1}{1-x} - 1 + \ln(1-x). \end{aligned}$$

APPENDIX B: BOUNDS FOR Γ_1

The index Γ_1 is bounded between 0 and 1. To show this, we will make use of L'Hôpital's rule. If $n = 1$ then $p_{11} = 1$ and Γ_1 has the indeterminate form 0/0, so by L'Hôpital's rule we have

$$\text{(B1)} \quad \lim_{n\to 1^+} \sum_{i=1}^{n}\sum_{j=1}^{n} \frac{p_{ij}^2 \ln(p_{ij})}{p_{ij}-1} = \lim_{p_{11}\to 1^-} \frac{p_{11} + 2p_{11}\ln(p_{11})}{1} = 1.$$

To establish the lower bound, consider that as $n \to \infty$ the p_{ij}s $\to$ 0. However, this results in the indeterminate form $0 \cdot \infty$. By writing $p_{ij}^2 \ln(p_{ij})$ as $\frac{\ln(p_{ij})}{1/p_{ij}^2}$ we obtain the indeterminate form ∞/∞ to which we can apply L'Hôpital's rule. Hence

$$\begin{aligned}
\text{(B2)} \quad \lim_{n\to\infty} \sum_{i=1}^{n}\sum_{j=1}^{n} \frac{p_{ij}^2 \ln(p_{ij})}{p_{ij}-1} &= \sum_{i=1}^{\infty}\sum_{j=1}^{\infty} \lim_{p_{ij}\to 0^+} \frac{\ln(p_{ij})}{1/p_{ij}^2}/(p_{ij}-1) \\
&= \sum_{i=1}^{\infty}\sum_{j=1}^{\infty} \lim_{p_{ij}\to 0^+} \frac{1/p_{ij}}{-2/p_{ij}^3}/(p_{ij}-1) \\
&= \sum_{i=1}^{\infty}\sum_{j=1}^{\infty} \lim_{p_{ij}\to 0^+} -\frac{p_{ij}^2}{2p_{ij}-2} \\
&= \sum_{i=1}^{\infty}\sum_{j=1}^{\infty} \frac{0}{2} = 0.
\end{aligned}$$

APPENDIX C: DELTA METHOD CALCULATIONS FOR VARIANCE OF $\hat{\Gamma}_1$ AND $\hat{\Gamma}_2$

Recall that n is defined as the number of land-cover categories. $\hat{\Gamma}_1$ and $\hat{\Gamma}_2$ are scalar statistics that are nonlinear functions of the n^2 elements of a $n \times n$ contingency table, where p_{ij} is the ijth element of the contingency table. As before, let Γ simultaneously represent Γ_1 and Γ_2. Let $\varepsilon_{ij} = (\hat{p}_{ij} - p_{ij})$ and $(\partial\Gamma/\partial p_{ij})_{|p_{ij}=\hat{p}_{ij}}$ be the partial derivative of Γ with respect to p_{ij} evaluated at $p_{ij} = \hat{p}_{ij}$. The first-order multivariate

Taylor series expansion of $\hat{\Gamma}$ is:

$$\text{(C1)}\quad \begin{aligned}\hat{\Gamma} \approx \Gamma &+ \varepsilon_{11}\left(\frac{\partial\Gamma}{\partial p_{11}}\right)_{|p_{11}=\hat{p}_{11}} + \cdots + \varepsilon_{1n}\left(\frac{\partial\Gamma}{\partial p_{1n}}\right)_{|p_{1n}=\hat{p}_{1n}} \\ &+ \varepsilon_{21}\left(\frac{\partial\Gamma}{\partial p_{21}}\right)_{|p_{21}=\hat{p}_{21}} + \cdots + \varepsilon_{2n}\left(\frac{\partial\Gamma}{\partial p_{2n}}\right)_{|p_{2n}=\hat{p}_{2n}} + \cdots \\ &+ \varepsilon_{n1}\left(\frac{\partial\Gamma}{\partial p_{n1}}\right)_{|p_{n1}=\hat{p}_{n1}} + \cdots + \varepsilon_{nn}\left(\frac{\partial\Gamma}{\partial p_{nn}}\right)_{|p_{nn}=\hat{p}_{nn}}.\end{aligned}$$

The Taylor series expansion in equation (C1) provides the following linear approximation:

$$\text{(C2)}\qquad \xi = \hat{\Gamma} - \Gamma \approx \sum_{i=1}^{n}\sum_{j=1}^{n}\varepsilon_{ij}\left(\frac{\partial\Gamma}{\partial p_{ij}}\right)_{|p_{ij}=\hat{p}_{ij}}.$$

The squared random error approximately equals ξ^2 from equation (C2):

$$\text{(C3)}\quad \begin{aligned}\xi^2 &\approx \left[\sum_{i=1}^{n}\sum_{j=1}^{n}\varepsilon_{ij}\left(\frac{\partial\Gamma}{\partial p_{ij}}\right)_{|p_{ij}=\hat{p}_{ij}}\right]\left[\sum_{k=1}^{n}\sum_{l=1}^{n}\varepsilon_{kl}\left(\frac{\partial\Gamma}{\partial p_{kl}}\right)_{|p_{kl}=\hat{p}_{kl}}\right] \\ &\approx \sum_{i=1}^{n}\sum_{j=1}^{n}\sum_{k=1}^{n}\sum_{l=1}^{n}\varepsilon_{ij}\varepsilon_{kl}\left(\frac{\partial\Gamma}{\partial p_{kl}}\right)_{|p_{kl}=\hat{p}_{kl}}\left(\frac{\partial\Gamma}{\partial p_{ij}}\right)_{|p_{ij}=\hat{p}_{ij}}.\end{aligned}$$

From equations (18) and (C3), the $\text{var}(\hat{\Gamma})$ is approximated as:

$$\text{(C4)}\quad \widehat{\text{var}}(\hat{\Gamma}) \approx \sum_{i=1}^{n}\sum_{j=1}^{n}\left(\frac{\partial\Gamma}{\partial p_{ij}}\right)_{|p_{ij}=\hat{p}_{ij}} E\left[\varepsilon_{ij}\varepsilon_{kl}\right]\sum_{k=1}^{n}\sum_{l=1}^{n}\left(\frac{\partial\Gamma}{\partial p_{kl}}\right)_{|p_{kl}=\hat{p}_{kl}}.$$

The covariances $E[\varepsilon_{ij}\varepsilon_{kl}]$ in equation (C4) can be determined using

equation (15). The values are as follows:

$$\text{(C5)} \quad \operatorname{cov}(\hat{p}_{ij}\hat{p}_{ij}) = \operatorname{var}(\hat{p}_{ij}) = E\left[\varepsilon_{ij}^2\right] - E^2\left[\varepsilon_{ij}\right] = \frac{\hat{p}_{ij}(1-\hat{p}_{ij})}{T},$$

$$\operatorname{cov}(\hat{p}_{ij}\hat{p}_{kl|kl\neq ij}) = E[\varepsilon_{ij}\varepsilon_{kl|kl\neq ij}] - E[\varepsilon_{ij}]E[\varepsilon_{kl|kl\neq ij}] = -\frac{\hat{p}_{ij}\hat{p}_{kl}}{T}.$$

Replacing the expectation in equation (C4) with the values from (C5) gives:

$$\text{(C6)} \quad \widehat{\operatorname{var}}(\hat{\Gamma}) \approx \frac{1}{T}\left\{\sum_{i=1}^{n}\sum_{j=1}^{n}\left[\left(\frac{\partial\Gamma}{\partial p_{ij}}\right)_{|p_{ij}=\hat{p}_{ij}}\right]^2 \hat{p}_{ij} - \sum_{i=1}^{n}\sum_{j=1}^{n}\left[\left(\frac{\partial\Gamma}{\partial p_{ij}}\right)_{|p_{ij}=\hat{p}_{ij}}\right]\hat{p}_{ij}\sum_{k=1}^{n}\sum_{l=1}^{n}\left[\left(\frac{\partial\Gamma}{\partial p_{kl}}\right)_{|p_{kl}=\hat{p}_{kl}}\right]\hat{p}_{kl}\right\}.$$

The first and second derivatives of Γ_1 at the point $(p_{11}, \ldots, p_{nn})$ are as follows:

$$\text{(C7)} \quad \frac{\partial\Gamma_1}{\partial p_{ij}} = \frac{p_{ij}^2\left[1+\ln(p_{ij})\right] - p_{ij}\left[1+2\ln(p_{ij})\right]}{(p_{ij}-1)^2};$$

$$\frac{\partial^2\Gamma_1}{\partial p_{ij}^2} = \frac{p_{ij}^2 - 4p_{ij} + 2\ln(p_{ij}) + 3}{(p_{ij}-1)^3}.$$

Substituting the derivative values from (C7) for the partial derivative notation in equation (C6) and simplifying gives:

$$\text{(C8)} \quad \widehat{\operatorname{var}}\left(\hat{\Gamma}_1\right) \approx \frac{1}{T}\left\{\sum_{i=1}^{n}\sum_{j=1}^{n}\hat{p}_{ij}\frac{\left[\hat{p}_{ij}^2\left(1+\ln(\hat{p}_{ij})\right) - \hat{p}_{ij}\left(1+2\ln(\hat{p}_{ij})\right)\right]^2}{(\hat{p}_{ij}-1)^4} - \left[\sum_{i=1}^{n}\sum_{j=1}^{n}\frac{\hat{p}_{ij}^3\left(1+\ln(\hat{p}_{ij})\right) - \hat{p}_{ij}^2\left(1+2\ln(\hat{p}_{ij})\right)}{(\hat{p}_{ij}-1)^2}\right]^2\right\}.$$

The first and second derivatives of Γ_2 at the point $(p_{11}, \ldots, p_{nn})$ are as follows:

$$\text{(C9)} \qquad \frac{\partial \Gamma_2}{\partial p_{ij}} = [1 + \ln(p_{ij})]; \quad \frac{\partial^2 \Gamma_2}{\partial p_{ij}^2} = p_{ij}^{-1}.$$

As before, substituting the derivative values from (C9) into equation (C6) and simplifying gives:

$$\text{(C10)} \quad \widehat{\text{var}}\left(\hat{\Gamma}_2\right) \approx \frac{\sum_{i=1}^{n}\sum_{j=1}^{n} \hat{p}_{ij} \ln^2(\hat{p}_{ij}) - \left[\sum_{i=1}^{n}\sum_{j=1}^{n} \hat{p}_{ij} \ln(\hat{p}_{ij})\right]^2}{T}.$$

ENDNOTES

1. The maximum-entropy principle (Shannon and Weaver [1949], Jaynes [1957]) provides a means to obtain least-biased statistical inference under uncertainty. The rule is to choose the probabilities so as to maximize the uncertainty when one has only partial information about the possible outcomes. In general, formulas for quantifying diversity and contagion have been motivated by information-theoretic axioms, i.e., the principle of entropy (Rényi [1961], Hill [1973], Ricotta et al. [2003]).

2. On a grid adjacency may be defined as sharing a common side ("rook's" definition, from chess), as sharing a corner ("bishop's" definition), or as either a side or corner ("queen's" definition). The standard used is rook's rule (O'Neill et al. [1988], Li and Reynolds [1993], Riitters et al. [1996]).

3. As a point of interest, it was shown (Section 4.3) that the second relative contagion index of Li and Reynolds [1993], known as RC_2, is a scaled version of Γ_2. The variance of $\widehat{RC_2}$, or $\hat{\Gamma}_{2(\text{scaled})}$, is simply the variance of $\hat{\Gamma}_2$ times the square of the scaling factor $2\ln(n)$, i.e.:

$$\begin{aligned}\widehat{\text{var}}(RC_2) &= \widehat{\text{var}}(\hat{\Gamma}_{2(\text{scaled})}) = \frac{\widehat{\text{var}}(\hat{\Gamma}_2)}{4\ln^2(n)} \\ &\approx \frac{\sum_{i=1}^{n}\sum_{j=1}^{n} \hat{p}_{ij} \ln^2(\hat{p}_{ij}) - [\sum_{i=1}^{n}\sum_{j=1}^{n} \hat{p}_{ij} \ln(\hat{p}_{ij})]^2}{4T\ln^2(n)}.\end{aligned}$$

4. Nationally, the FIA program collects data on sample plots spaced across each state on a 3- by 3-mile (4.8- by 4.8-km) grid. Detailed descriptions of the southern FIA data can be found in May [1990].

5. In ecology, dominance or concentration is normally measured using some function of p_i^2 as this has been shown to reflect expected commonness (see Pielou [1975, pp. 8–9]). Note that Γ_1 is a function of p_{ij}^2.

6. The true entropy index of contagion is Γ_2; and RC_2, the scaled or relativized version of Γ_2, is its corresponding "evenness/configuration" index.

REFERENCES

M. Alberti [2009], *Advances in Urban Ecology: Integrating Humans and Ecological Processes in Urban Ecosystems*, Springer, New York.

Y.M.M. Bishop, S.E. Fienberg, and P.W. Holland [1975], *Discrete Multivariate Analysis: Theory and Practice*, MIT Press, Cambridge, MA.

R.L. Burgess and D.M. Sharpe, eds. [1981], *Forest Island Dynamics in Man-Dominated Landscapes*, Springer-Verlag, New York.

V.H. Dale, F. Southworth, R.V. O'Neill, A. Rosen, and R. Frohn [1993], *Simulating Spatial Patterns of Land-use Change in Rondônia, Brazil*, Lect Math Life Sci **23**, 29–55.

V.H. Dale, R.V. O'Neill, F. Southworth, and M. Pedlowski [1994], *Modeling in the Brazilian Amazonian Settlement of Rondônia*, Conserv Biol **8**, 196–206.

C. Dietzel, M. Herold, J.J. Hemphill, and K.C. Clarke [2005], *Spatio-temporal Dynamics in California's Central Value: Empirical Links to Urban Theory*, Int J Geogr Inform Sci **19**(2), 175–195.

F.H. Eyre, ed. [1980], *Forest Cover Types of the United States and Canada*, Society of American Foresters, Washington, DC.

W. Feller [1968], *An Introduction to Probability Theory and its Applications*, Vol. I, 3rd ed., Section II.7: *Examples for Waiting Times*, Wiley, New York, pp. 47–50.

J.S. Fralish and S.B. Franklin [2002], *Taxonomy and Ecology of Woody Plants in North American Forests*, Wiley, New York.

R.C. Frohn [1998], *Remote Sensing for Landscape Ecology: New Metric Indicators for Monitoring, Modeling, and Assessment of Ecosystems*, Lewis Publishers, Boca Raton, FL.

R.L. Graham, C.T. Hunsaker, R.V. O'Neill, and B. Jackson [1991], *Ecological Risk Assessment at the Regional Scale*, Ecological Application **1**, 196–206.

E.J. Gustafson and G.R. Parker [1992], *Relationships between Landcover Proportion and Indices of Landscape Spatial Pattern*, Lanscape Ecology **7**, 101–110.

B.N. Haack and A. Rafter [2006], *Urban Growth Analysis and Modeling in the Kathmandu Valley, Nepal*, Habitat International **30**(4), 1056–1065.

M.O. Hill [1973], *Diversity and Evenness: A Unifying Notation and Its Consequences*, Ecology **54**, 427–431.

E.J. Hodgkins, M.S. Golden, and W.F. Miller [1979], *Forest Habitat Regions and Types on a Photomorphic-Physiographic Basis: A Guide to Forest Site Classification in Alabama-Mississippi*, Southern Cooperative Series No. 210, Alabama Agricultural Experiment Station, Auburn University, Auburn, AL.

E.T. Jaynes [1957], *Information Theory and Statistical Mechanics*, Phys. Rev. **106**, 620–630.

G.G. Judge, R.C. Hill, W.E. Griffiths, H. Lütkepohl, and T. Lee [1988], *Introduction to the Theory and Practice of Econometrics*, 2nd ed., Wiley, New York.

M. Kachmar, G.A. Sánchez-Azofeifa, B. Rivard, and Y. Kakubari [2005], *Improved Forest Cover Classification in an Industrialized Mountain Area in Japan*, Mountain Research and Development **25**(4), 349–356.

O. Kempthorne and L. Folks [1971], *Probability, Statistics, and Data Analysis*, The Iowa State University Press, Ames, IA.

H. Li and J.F. Reynolds [1993], *A New Contagion Index to Quantify Spatial Patterns of Landscapes*, Landscape Ecol. **8**, 155–162.

D.M. May [1990], *Stocking, Forest Type, and Stand Size Class–the Southern Forest Inventory and Analysis Unit's Calculation of Three Important Stand Descriptors*, General Technical Report SO-77, U.S. Department of Agriculture, Forest Service, Southern Forest Experiment Station, New Orleans, LA.

P.D. Miles, G.J. Brand, C.L. Alerich, L.F. Bednar, S.W. Woudenberg, J.F. Glover, and E.N. Ezzell [2001], *The Forest Inventory and Analysis Database: Database Description and Users Manual Version 1.0*, General Technical Report NC-218, U.S. Department of Agriculture, Forest Service, North Central Research Station, St. Paul, MN.

R.V. O'Neill, J.R. Krummel, R.H. Gardner, G. Sugihara, B. Jackson, D.L. DeAngelis, B.T. Milne, M.G. Turner, B. Zygmont, S.W. Christensen, V.H. Dale, and R.L. Graham [1988], *Indices of Landscape Pattern*, Landscape Ecol. **1**, 153–162.

R.K. Peet [1975], *Relative Diversity Indices*, Ecology **56**, 496–498.

E.C. Pielou [1975], *Ecological Diversity*, Wiley, NY.

C.R. Rao [1965], *Linear Statistical Inference and Its Applications*, Wiley, NY.

M.V. Ratnaparkhi [1985], *Multinomial Distributions*, Encyclopedia of Statistical Sciences **5**, 659–665, Wiley, New York.

A. Rényi [1961], *On Measures of Entropy and Information*, Berkeley Symposium on Mathematical Statistics and Probability **4**, 547–561.

C. Ricotta, P. Corona, and M. Marchetti [2003], *Beware of Contagion!*, Landscape and Urban Planning **62**, 173–177.

K.H. Riitters, R.V. O'Neill, J.D. Wickham, and K.B. Jones [1996], *A Note on Contagion Indices for Landscape Analysis*, Landscape Ecol. **11**, 197–202.

D.L. Sachs, P. Sollins, and W.B. Cohen [1998], *Detecting Landscape Changes in the Interior of British Columbia from 1975 to 1992 Using Satellite Imagery*, Can. J. Forest Res. **28**, 23–36.

S.L. Salas and E. Hille [1974], *Calculus: One and Several Variables*, 2nd ed., Wiley, New York.

N. Sasaki, K. Takejima, T. Kusakabe, and T. Sweda [2001], *Forest Cover Classification Using Landsat Thematic Mapper Data for Areal Expansion of Line LAI Estimate Generated through Airborne Laser Profile*, Polar Biosci. **14**, 110–121.

C.E. Shannon and W. Weaver [1949], *The Mathematical Theory of Communication*, University of Illinois Press, Urbana.

R.M. Sheffield, N.D. Cost, W.A. Bechtold, and J.P. McClure [1985], *Pine Growth Reductions in the Southeast*, Resource Bulletin SE-83, U.S. Department of Agriculture, Forest Service, Southeastern Forest Experiment Station, Asheville, NC.

A.L. Sheldon [1969], *Equitability Indices: Dependence on the Species Count*, Ecology **50**, 466–467.

L.R. Shenton and K. Hutcheson [1969], *Moments of Moments and Frequencies: Expectation of Power-sums Related to Categorized Data*, Technical Reprint Series **17**, 7–39, University of Georgia Computer Center, Athens, GA.

X. Shi, F. Hao, C. Zhao, D. Wang, and W. Ouyang [2008], *Landscape Dynamics Analysis of Guide Wetlands in Yellow River Watershed by Landsat Series Data*, The International Archives of the Photogrammetry, Remote Sensing and Spatial Information Sciences **37**(Part B2), 247–252.

R.B. Thapa and Y. Murayama [2008], *Spatial Structure of Land Use Dynamics in Kathmandu Valley*, The International Archives of the Photogrammetry, Remote Sensing and Spatial Information Sciences **37**(Part B8), 11–16.

C.E. Thomas and B.R. Parresol [1989], *Comparing Basal Area Growth Rates in Repeated Inventories: Simpson's Paradox in Forestry*, Forest Science **35**(4), 1029–1039.

M.G. Turner [1989], *Landscape Ecology: The Effect of Pattern on Process*, Annu. Rev. Ecol. Syst. **20**, 171–197.

M.G. Turner and C.L. Ruscher [1988], *Changes in Landscape Patterns in Georgia, USA*, Landscape Ecol. **1**, 241–251.

R.H. Waring and S.W. Running [1998], *Forest Ecosystems: Analysis at Multiple Scales*, 2nd ed., Academic Press, San Diego, CA.

X. Yu and C. Ng [2006], *An Integrated Evaluation of Landscape Change Using Remote Sensing and Landscape Metrics: A Case Study of Panyu, Guangzhou*, Int. J. Remote Sensing **27**(6), 1075–1092.

B. Zeide [1992], *Has Pine Growth Declined in the Southeastern United States?*, Conserv. Biol. **6**(2), 185–195.

Z. Zhu and D.L. Evans [1994], *U.S. Forest Types and Predicted Percent Forest Cover from AVHRR Data*, Photogramm. Eng. Remote Sens. **60**(5), 525–531.